Analysis of Conflict Risk in Terminal Maneuvering Area using Recorded ADS-B Trajectories

Hyeonwoong Lee*, Bae-Seon Park, HeeGyeong Lyu, and Hak-Tae Lee**

Department of Aerospace Engineering, Inha University, Incheon, Republic of Korea

Abstract

An Automatic Dependent Surveillance-Broadcast (ADS-B) receiver has been installed at Inha University in 2016. The location of Inha University, being near Incheon International Airport and Gimpo International Airport, allows the ADS-B receiver to cover the most congested airspace in the Republic of Korea. In this paper, a risk analysis is performed by calculating Conflict Intrusion Parameter (CIP) and Well Clear (WC) using the recorded ADS-B data. Data accumulated for one week from April 20th to 26th, 2017 are used for the analyses. Due to poor reception at various time intervals, some aircraft trajectories contain missing segments. These segments were reconstructed by interpolation within a reliable reception range to complete the overall aircraft trajectory. In order to synchronize the time between trajectories, the update cycle of all trajectory is set to one second and the points are resampled. Since the recorded ADS-B data belongs to aircraft that are already separated and managed by air traffic controllers, the risk analyzed by applying the standard separation cannot capture the risk properly. Therefore, the data were analyzed using relaxed separation criteria, which are constructed by multiplying various relaxation factors to the standard separation criteria. CIP analyses confirmed that the aircraft were generally properly separated except at low altitudes near airports. Using relaxation factors, the time intervals and regions of potential risk could be identified, which are mostly near the final arrival path to Incheon International Airport and Gimpo International Airport. WC analyses showed better correlation with the actual risk, since it also accounts for relative velocity and time. Many of the air route merge points were identified as the potential risk area using the WC analyses. The risk analyses will be the bases of the studies on various next generation air traffic management concepts, including the integration of the unmanned aircraft system.

Keywords: Automatic Dependent Surveillance–Broadcast (ADS-B), Risk Analysis, Well Clear (WC), Conflict Intrusion Parameter (CIP)

Nomenclature

r_{xy}	=	horizontal separation
S_{std}	=	horizontal separation standard
d_h	=	vertical separation
H_{std}	=	vertical separation standard
h_i	=	altitude
HMD	=	horizontal miss distance
d_x	=	horizontal separation in the x-direction
d_y	=	horizontal separation in the y-direction
v_{rx}	=	relative horizontal velocity in the x-dimension
v_{ry}	=	relative horizontal velocity in the y-dimension
t_{CPA}	=	time to horizontal closest point of approach
τ_{mod}	=	modified tau
$\dot{r}_{xy}$	=	horizontal range rate
$DMOD$	=	distance modification of modified tau
τ^*_{mod}	=	modified tau threshold
HMD^*	=	horizontal miss distance threshold
d^*_h	=	vertical separation threshold

1. Introduction

With the continuously increasing demand for air travel, the number of airborne flights are keep increasing causing various unpredictable and complicated situations in the airspace. This increased aircraft density leads to higher probability of airborne conflicts and collisions. Therefore, risk analyses are needed to manage the airspace safely and efficiently. An ADS-B receiver was installed at Inha University in 2016, and it is collecting track data daily. Inha University is located between Incheon International Airport (RKSI) and Gimpo International Airport (RKSS). Consequently, the receiver covers Seoul Traffic Maneuvering Area (TMA) and its surroundings, the busiest airspace in the Republic of Korea. About 1,100 trajectory data are collected and processed each day and stored in a database system so that the data can be used not only for traffic analyses but also for various air traffic simulations [1].

In this paper, risk analyses were performed using collected ADS-B data around the Seoul TMA. The risk metrics utilized in the study are CIP [2], and WC [3]. CIP is a distance based conflict risk metric. WC is a new metric introduced for unmanned aircraft that is adapted from the Traffic Collision Avoidance System. WC considers relative velocities and times. Using these two metrics and various separation standards, potential risk area in the Seoul TMA are identified. As can be expected, the risk area are concentrated around the final arrival paths and air route merge points. In the future, these data can be used to improve the routes and procedures, especially for new kinds of aircraft such as unmanned aircraft.

2. ADS-B Data

* Presenting Author: Graduate Student, 22161558@inha.edu, Member, KSAS.
** Corresponding Author: Professor, haktae.lee@inha.ac.kr, Member, KSAS.

2.1. Data reception range

Data reception range of the ADS-B receiver is influenced by the location of the antenna and the surrounding environment. The receiver used in this study can receive up to 210 NMI to the West (The Yellow Sea), up to 120 NMI to the South (Jeongeup, Jeollabuk-Do), and up to 160 NMI to the North (Taebaek, Gangwon-Do).

Fig. 1 shows all the track data collected for one week from April 20th to 26th, 2017. Fig. 2 shows tracks around RKSI and RKSS, which reveals frequently used routes.

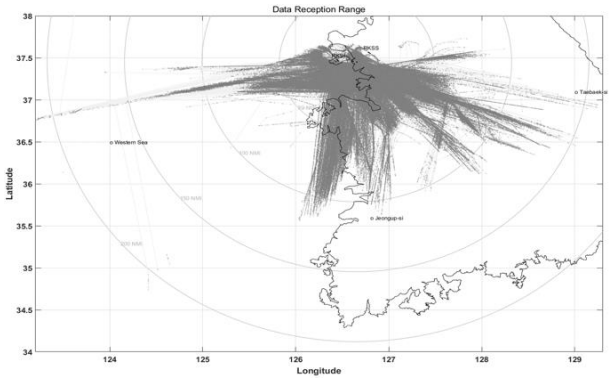

Fig. 1. Reception range of the ADS-B receiver

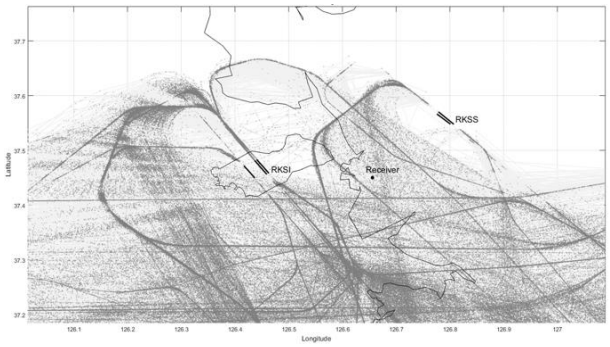

Fig. 2. Tracks around RKSI and RKSS

2.2. Data processing

ADS-B data consist of two components, position data and state data. Position data refers to latitude, longitude, and altitude, and state data refers to velocity and track angle. There is a time difference between the two data [1]. Therefore, it is necessary to compensate for this time difference between aircraft's position data and state data to create a single-track point. These track points are generated by flight, each consisting of time, latitude, longitude, altitude, speed, and track angle. Table 1 is an example of the trajectory data.

TIME column in Table 1 shows that the time interval is irregular. Due to intermittent no reception time intervals, some track data contain missing segments. Calculation of risk involves comparing the positions of aircraft at a given time instance. Therefore, it is necessary to interpolate the missing intervals and resample the track data at a regular time interval.

Table 1. Trajectory data

TPN	*LAT (deg)*	*LON (deg)*	*Spd* (kts)*	*ALT (ft)*	*TIME (hh:mm:ss)*	*TrkAng* (deg)*
TP1	37.02365	127.6327	323	18000	**21:05:51**	306
TP2	37.02458	127.6310	323	18000	**21:05:52**	306
TP3	37.02923	127.6227	322	18000	**21:05:57**	306
TP4	37.03016	127.6210	322	18000	**21:05:58**	306
TP5	37.03374	127.6146	320	18000	**21:06:12**	306
TP6	37.03400	127.6142	320	18000	**21:06:13**	306
TP7	37.03774	127.6075	320	18000	**21:06:16**	306
TP8	37.04399	127.5963	320	18000	**21:06:21**	306
TP9	37.04523	127.5941	320	18000	**21:06:22**	306
TP10	37.04648	127.5918	320	18000	**21:06:23**	306

Spd*: Speed, TrkAng*: Track Angle

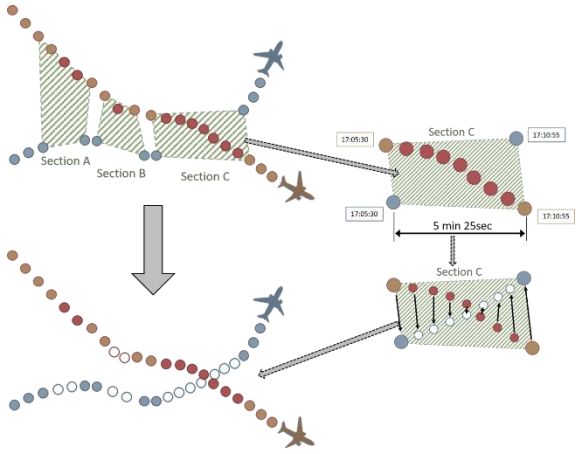

Fig. 3. Interpolation and time synchronization

Fig. 3 shows the time synchronization and interpolation of the two aircraft tracks. All track data are resampled at one-second interval. Finally, the data are sorted by time. Table. 2 shows part of the sorted track data.

Table 2. Sorted trajectory data

Date Time	**Flights**	***Flight Data (ICAOaddress/CallSign/Lat/Lon/Alt/Speed/Track)***		
		1st Flight	***2nd Flight***	***3rd Flight ⋯***
2017/04/20 00:24:55	3	71BE24/KAL283/ 37.3296/126.4789/ 11937/410/109	86D943/AJX8480/ 37.4350/126.3049/ 12158/374/155	06A066/QTR807/ 37.4090/126.1881/ 30000/406/270
2017/04/20 00:24:56	3	71BE24/KAL283/ 37.3290/126.4811/ 11968/410/108	86D943/AJX8480/ 37.4332/126.3059/ 12194/374/155	06A066/QTR807/ 37.4090/126.1861/ 30000/406/270
2017/04/20 00:24:57	3	71BE24/KAL283/ 37.3284/126.4833/ 12000/411/108	86D943/AJX8480/ 37.4315/126.3069/ 12230/375/155	06A066/QTR807/ 37.4090/126.1842/ 30000/406/270
2017/04/20 00:24:58	3	71BE24/KAL283/ 37.3282/126.4844/ 12025/412/106	86D943/AJX8480/ 37.4298/126.3079/ 12266/376/155	06A066/QTR807/ 37.4090/126.1823/ 30000/406/270

2017/04/20 00:24:59	3	71BE24/KAL283/ 37.3278/126.4864/ 12050/412/105	86D943/AJX8480/ 37.4281/126.3089/ 12302/376/155	06A066/QTR807/ 37.4090/126.1804/ 30000/406/270
2017/04/20 00:25:00	2	71BE24/KAL283/ 37.3273/126.4884/ 12075/412/105	86D943/AJX8480/ 37.4264/126.3099/ 12338/377/155	-
2017/04/20 00:25:01	2	71BE24/KAL283/ 37.3269/126.4904/ 12100/412/105	86D943/AJX8480/ 37.4247/126.3109/ 12375/378/155	-

3. Analysis of Conflict Risk

Risk analysis uses two metrics, CIP and WC. Since both the metrics are based on the currently used separation management standards, and the recorded track data are the tracks already managed by air traffic controllers, chances of violating the separation standard is extremely small. To identify the trends and compare the relative risk of properly separated aircraft, separation standards are multiplied by various relaxation factors. Risk metrics are reevaluated by substantially increasing the separation standard up to 3.5 times.

3.1. Conflict Intrusion Parameter

CIP calculates risk using the horizontal and vertical distance between the two aircraft as described in Eq. (1) [2].

$$CIP(r_{xy}, d_h) = 1 - 0.5 \times \left\{ \min_{t_{loc} \le t \le t_{eoc}} \left(\frac{r_{xy}}{S_{std}} + \frac{d_h}{H_{std}} \right) \right\} \quad (1)$$

If horizontal and vertical distances are zero, CIP is one, which means collision. If the horizontal and vertical distances between the two aircraft are greater than the separation standards, it is zero, which indicates that there is no conflict between the two aircraft. Since the data are processed at a regular one-second interval, Eq. (1) can be modified as shown in Eq. (2) [4].

$$CIP(r_{xy}, d_h) = \max \left\{ 1 - 0.5 \times \left(\frac{r_{xy}}{S_{std}} + \frac{d_h}{H_{std}} \right), 0 \right\} \quad (2)$$

Table 3 shows modified separation standard by multiplying relaxation factors to the standard separation values, which are five nmi horizontally and 1,000 ft vertically.

Table 3. Modified separations for CIP

Variable	*FAA Separation*	*Factor*	*Modified Separation*
S_{std}	5 nmi	1.0	5 nmi
		1.5	7.5 nmi
		2.0	10 nmi
		2.5	12.5 nmi
		3.0	15 nmi
		3.5	17.5 nmi
H_{std}	1000 ft	1.0	1000 ft
		1.5	1500 ft
		2.0	2000 ft
		2.5	2500 ft
		3.0	3000 ft
		3.5	3500 ft

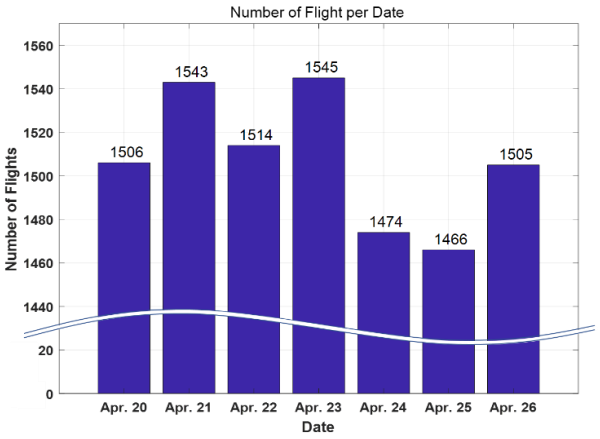

Fig. 4. Number of flights per date

Fig. 4 shows the number of aircraft per day in the collected data. April 23rd has the largest number of flights for the week. CIP was calculated for April 23rd according to the modified standards.

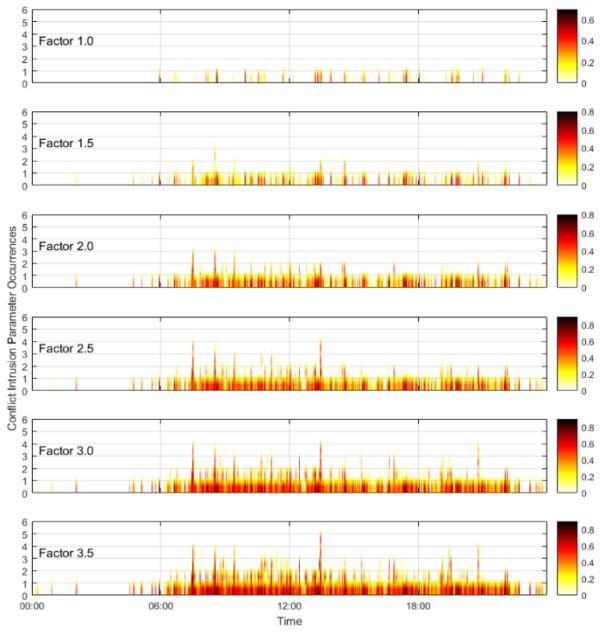

Fig. 5. CIP occurrences and values (April 23rd, 2017)

Fig. 5 shows the CIP computed by each modified separation standard. The x-axis represents time of the day, and the y-axis indicates the number of times the CIP value is greater than zero. Additionally, it is possible to check the

CIP values for each conflict through the color bar.

Fig. 5 indicates that there are significant number of cases of standard separation being violated. Fig. 6 shows the values and locations of those points of violation. The circles are placed at the midpoint between the two aircraft that has CIP greater than zero.

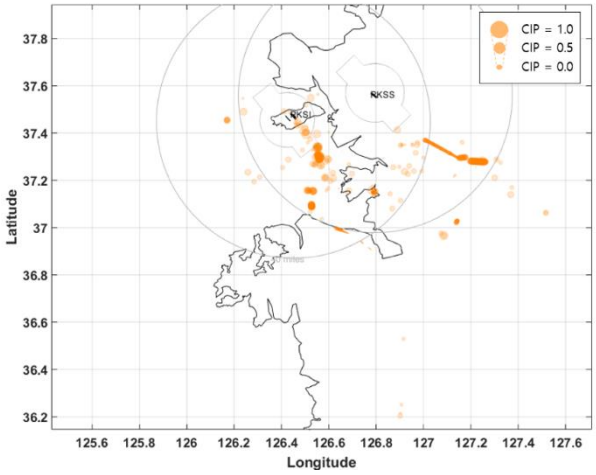

Fig. 6. Regions of conflict (April 23rd, 2017)

Most of these circles are inside the Class B airspaces of the RKSI and the RKSS. In Class B airspace, it is not appropriate to calculate the risk based only on distances because most aircraft fly along sophisticated routes that are part of takeoff, landing, and approach procedures. Nevertheless, the circled areas shown in Fig. 6 indicate regions with relatively higher risk. For example, when adding new arrival routes for unmanned aircraft, it may be better to avoid these areas. Outside the Class B airspaces, only a few aircraft pairs show the CIP values exceeding zero for only several seconds.

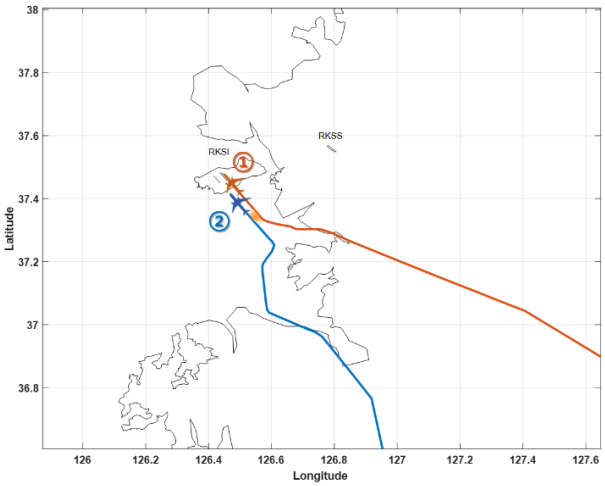

Fig. 7. Position of the conflict pair with the largest value of CIP

Fig. 7 shows the trajectories and positions of the two aircraft of highest CIP value at 17:27. In this case, the altitude of the two aircraft are equal, and the horizontal distance is 2.31 NMI. Aircraft 1 is an Airbus 330-300, landing on the runway 33R of the RKSI. Aircraft 2 is a Boeing 737-800, landing on the runway 34 of the same airport. The distance between the two runways is about 8,200 feet, indicating that independent operation is possible. So, the situation described in Fig. 7 is normal and is not a safety concern.

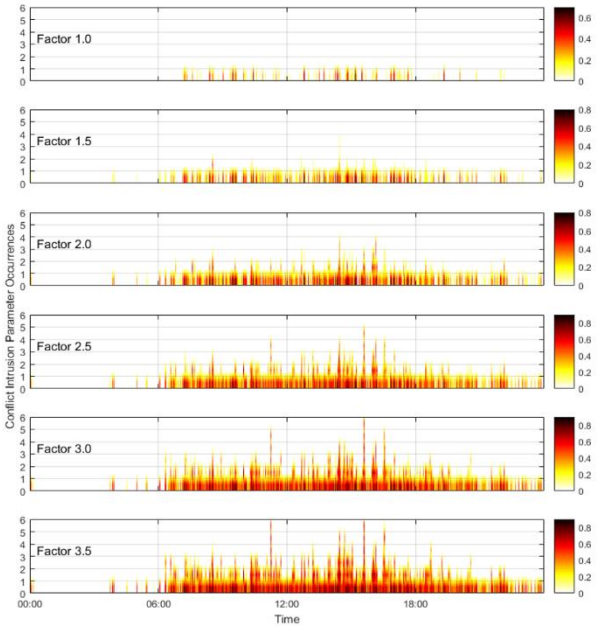

Fig. 8. CIP occurrences and values (April 24th, 2017)

Fig. 8 shows the results of CIP calculation on April 24th, 2017. With the factor of 3.5, six pairs of aircraft simultaneously showed conflict four times during the 24-hour period. Those values can be found in Table 4.

Table 4. CIP value of each time – factor 3.5

Time	*CIP value*	*Time*	*CIP value*
11:15:19	0.3949	**15:35:51**	0.1617
	0.5519		0.3922
	0.0244		0.3814
	0.3418		0.6962
	0.1712		0.3599
	0.6802		0.6637
14:27:23	0.0436	**16:32:08**	0.1667
	0.4419		0.3741
	0.4205		0.1840
	0.5648		0.3030
	0.0632		0.5716
	0.0102		0.1584

Among the six conflict pairs in Table 4, the one at 15:35 show particularly high values of CIP. Fig. 9 shows the

positions and the values of the CIP for the six pairs. The conflicts are caused by one aircraft arriving at RKSI and three aircraft departing from RKSS. The result suggests that there is a potential danger near an area where departure from one airport and arrival to another airport cross over.

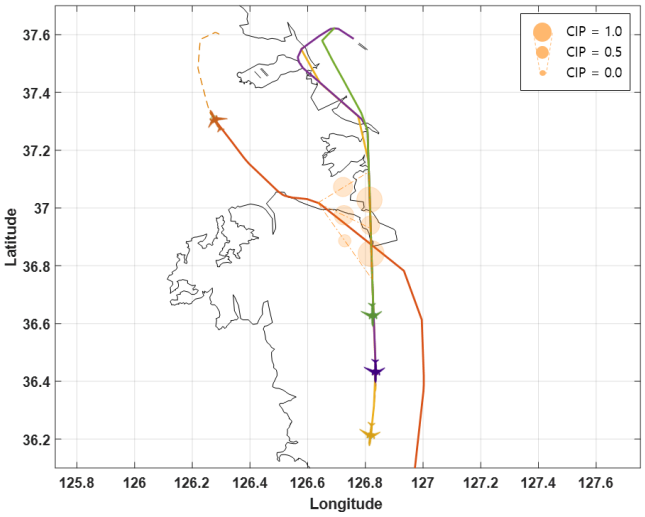

Fig. 9. CIP occurrences at 15:35:51, April 23rd, 2017

Figs. 10 - 16 represent the values of the CIPs and the locations of the conflicts with various relaxation factors for one week. Except for the white background, smaller yellow circles represent lowest risk area. As the color of the circle turns closer to red and as the size of the circle gets larger, the risk increases. Generally, higher risk areas appear as lines that go over the runways aligned with the runway directions. However, significant daily variations can also be observed.

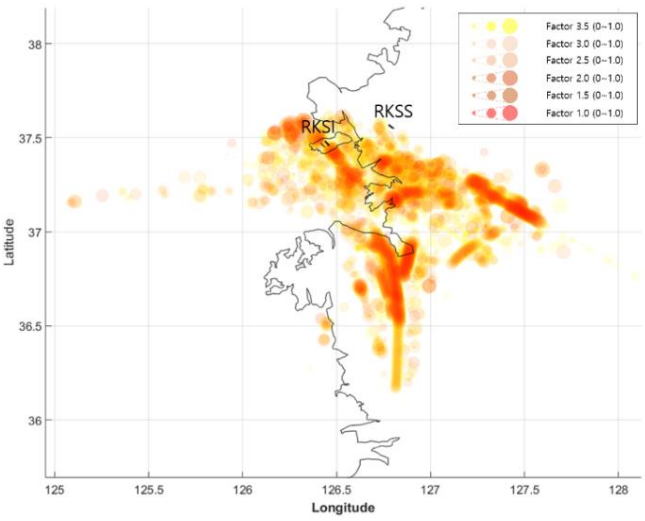

Fig. 10. CIP locations by factor (April 20th, 2017)

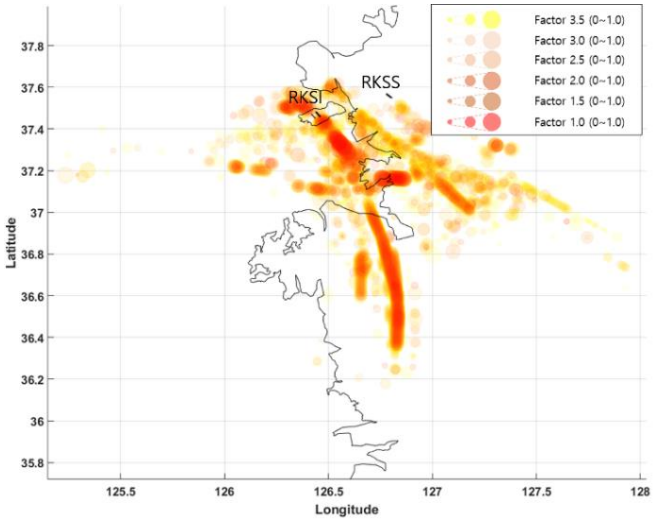

Fig. 11. CIP locations by factor (April 21st, 2017)

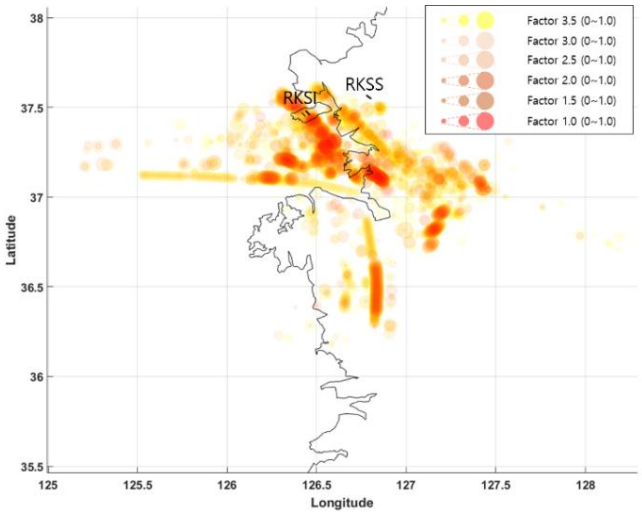

Fig. 12. CIP locations by factor (April 22nd, 2017)

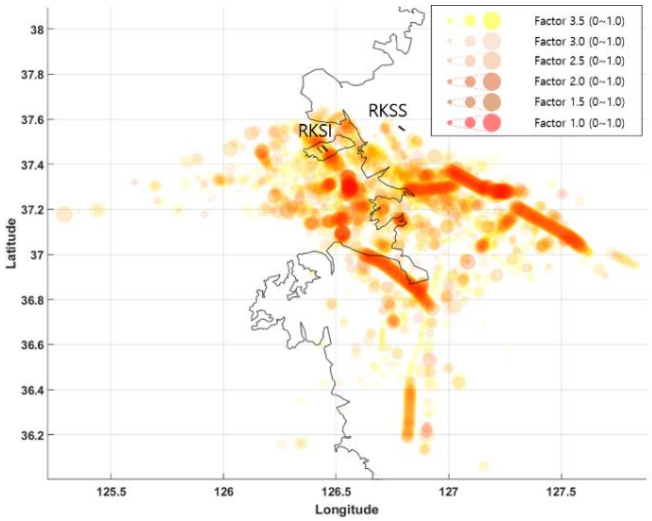

Fig. 13. CIP locations by factor (April 23rd, 2017)

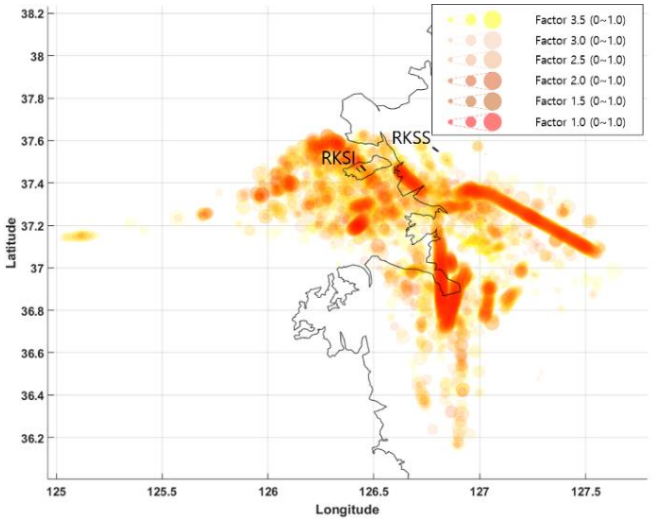

Fig. 14. CIP locations by factor (April 24th, 2017)

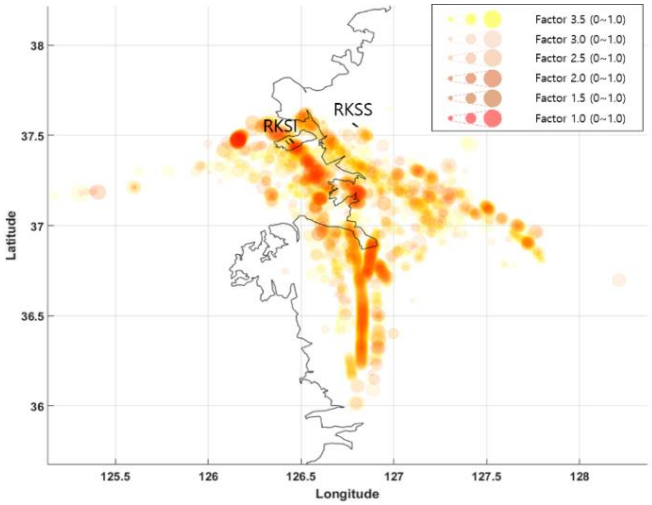

Fig. 15. CIP locations by factor (April 25th, 2017)

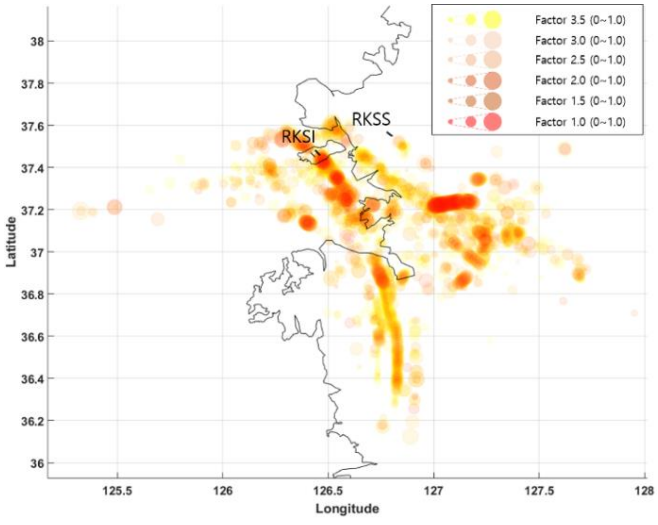

Fig. 16. CIP locations by factor (April 26th, 2017)

3.2. Well Clear

WC is a newly introduced metric to mathematically define the concept of "well clear" that has not been quantified in the regulations for manned aircraft. It was devised to be used with the Detect and Avoid (DAA) system of unmanned aircraft system to handle the risks in between conflict and collision [6].

Using the locations and velocities of two aircraft [3], the WC calculates the risk using three parameters, vertical separation at the current time, d_h, horizontal miss distance at the moment of horizontal closest point of approach, HMD, and the modified tau, τ_{mod}. Eqs. (3) - (4) show how these parameters are calculated [6].

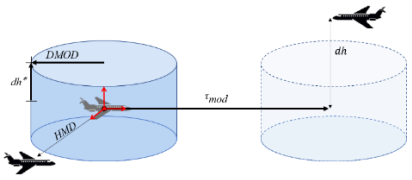

Fig. 17. Schematic of parameters used to well clear

$$HMD = \begin{cases} \sqrt{(d_x + v_{rx}t_{CPA})^2 + (d_y + v_{ry}t_{CPA})^2} & for \;\; t_{CPA} \geq 0 \\ -\infty & for \;\; t_{CPA} < 0 \end{cases}$$

$$where$$

$$d_x = x_2 - x_1, \;\; d_y = y_2 - y_1, \;\; v_{rx} = \dot{x}_2 - \dot{x}_1, \;\; v_{ry} = \dot{y}_2 - \dot{y}_1 \tag{3}$$

$$t_{CPA} = -\frac{d_x v_{rx} + d_y v_{ry}}{v_{rx}^2 + v_{ry}^2}$$

$$\tau_{\mathrm{mod}} = \begin{cases} 0 & when \; r_{xy} \leq DMOD \\ -\dfrac{(r_{xy}^2 - DMOD^{2})}{r_{xy}\dot{r}_{xy}} & when \; r_{xy} > DMOD \;\; and \;\; \dot{r}_{xy} < 0 \\ \infty & when \; r_{xy} > DMOD \;\; and \;\; \dot{r}_{xy} < 0 \end{cases} \tag{4}$$

$$where$$

$$r_{xy}\sqrt{d_x^2 + d_y^2}, \;\; \dot{r}_{xy} = \frac{d_x v_{rx} + d_y v_{ry}}{r_{xy}}$$

These three values are compared to the conditions in Table 5 to determine if Loss of Well Clear (LoWC) has happened. Generally, the requirement for the DAA system is such that it must always prevent LoWC situation. For the risk level lower than LoWC, the alert levels can be determined using the conditions in Table 6.

Table 5. Condition of LoWC

	LoWC	***Standard Value***
τ_{mod}	$0 \leq \tau_{\mathrm{mod}} \leq \tau_{\mathrm{mod}}^{*}$	$\tau_{\mathrm{mod}}^{*} = 35\,\mathrm{sec}$
HMD	$0 \leq HMD \leq HMD^{*}$	$HMD^{*} = 4{,}000\;ft$
d_h	$d_h \leq d_h^{*}$	$d_h^{*} = 450\;ft$

Table 6. WC self-separation alert level [2]

Standard Value	*Advisory*	*Preventative Caution*	*Corrective Caution*	*Warning*
Within Time	60 sec	55 sec	55 sec	40 sec
τ^*_{mod}	35 sec	35 sec	35 sec	35 sec
HMD^*	2.0 nmi	0.66 nmi	0.66 nmi	0.66 nmi
d^*_h	1,200 ft	700 ft	450 ft	450 ft

In addition, another metric called Severity of Loss of DAA Well clear (SLoWC) is proposed to quantify the level of risk between LoWC and collision [6]. SLoWC is calculated using Eqs. (5) - (11).

$$SLoWC = (1 - RangePen \oplus HMDPen \oplus VertPen) \times 100\% \quad (5)$$

$$x \oplus y \equiv \sqrt{x^2 + (1 - x^2) \cdot y^2} \quad (6)$$

$$RangePen = MIN\left(\frac{r}{S}, 1\right) \quad (7)$$

$$S = MAX\left\{DMOD, \frac{1}{2} \cdot \left\{\sqrt{\left(\dot{r} \cdot \tau^*_{mod}\right)^2 + 4 \cdot DMOD^2} - \dot{r} \cdot \tau^*_{mod}\right\}\right\} \quad (8)$$

$$HMDPen = MIN\left(\frac{HMD}{DMOD}, 1\right) \quad (9)$$

$$HMD = \begin{cases} \sqrt{(d_x + v_{rx} t_{CPA})^2 + (d_y + v_{ry} t_{CPA})^2} & (t_{CPA} > 0) \\ r_{xy} & (t_{CPA} \le 0) \end{cases} \quad (10)$$

$$VertPen = MIN\left(\frac{d_h}{H^*}, 1\right) \quad (11)$$

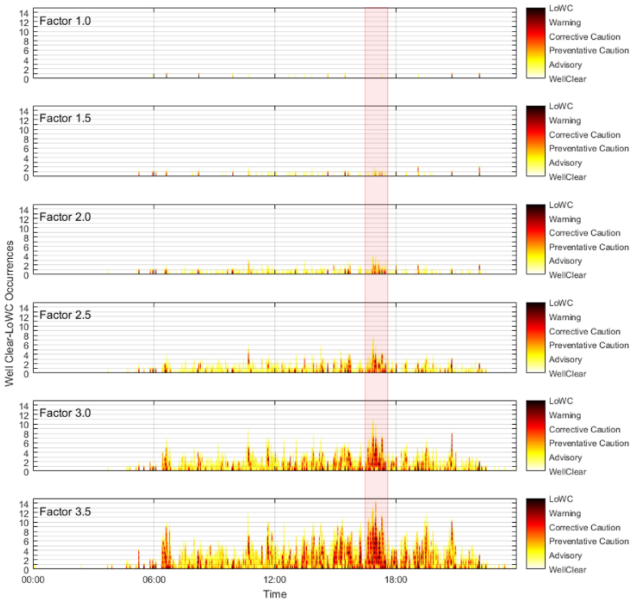

Fig. 18. Level of well clear alerts (April 23rd, 2017)

As shown in Equation (5), the SLoWC represents a percentage, and the higher the risk, the closer it is to 100 %.

Similar to CIP, manned aircraft traffic managed by air traffic controllers showed risk levels up to LoWC infrequently. Relaxation factor were applied to the standards in Tables 5 and 6 to examine the trend.

Fig. 18 shows the number of alerts and the corresponding levels with respect to time with relaxation factors from one to 3.5 on April 23rd, 2017. It can be observed that WC alerts show less risk than the CIP of Fig. 5. The results show that risk metric that considers relative velocity and time is better aligned with the actual risk situation near airports.

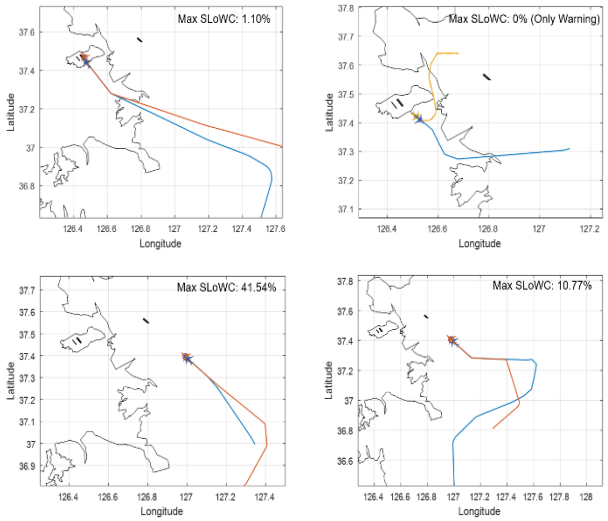

Fig. 19. Trajectories of LoWC level at factor 1.0

A total of four incidences of LoWC were detected using the relaxation parameter of one. Fig. 19 shows those four trajectories on the map. In all four cases, warning level alerts happened at the beginning of the climb from the airport or landing to the airport below 2,500 ft. Due to the ambient environment around the antenna, the data were often susceptible to poor reception below 2,500ft. Therefore, this result requires further investigation.

For about an hour and thirty minutes from 16:00 to 17:30, relatively high levels of risk is observed from the relaxation factor 3.5 case in Fig. 18. Compared to the CIP of Fig. 8 that does not show notable differences with respect to time, WC alerts show larger variations depending on the time of the day.

Fig. 20 shows the alert levels of risk during the 1.5-hour period on the map. The locations of the alerts are mostly concentrated near the merge point of approach routes to the airport.

Figs. 21 - 27 show the alert of risk levels and SLoWC on the map. Similar to CIP, the risk based Well Clear is shown in the form of concentration near the airport and the around the airport.

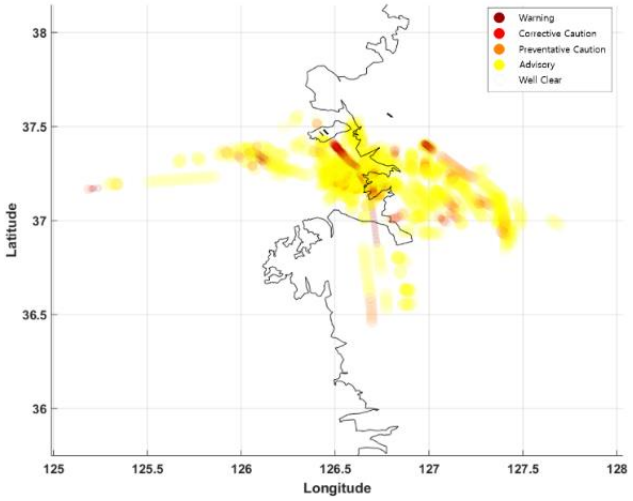

Fig. 20. WC alert levels from 16:00:00 to 17:30:00, April 23rd, 2017

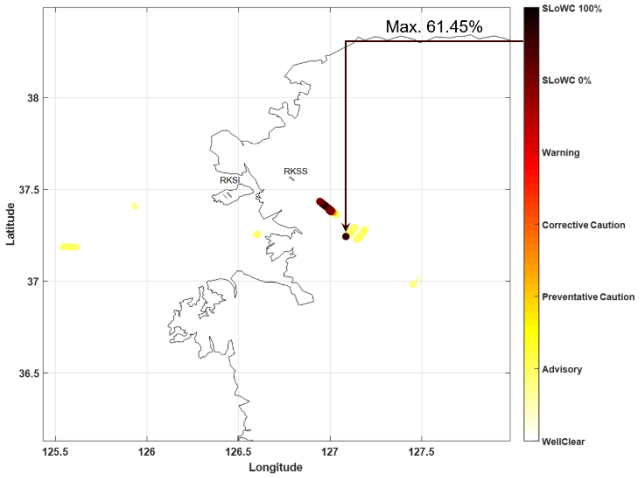

Fig. 21 LoWC and SLoWC - Factor 1.0 (April 20th, 2017)

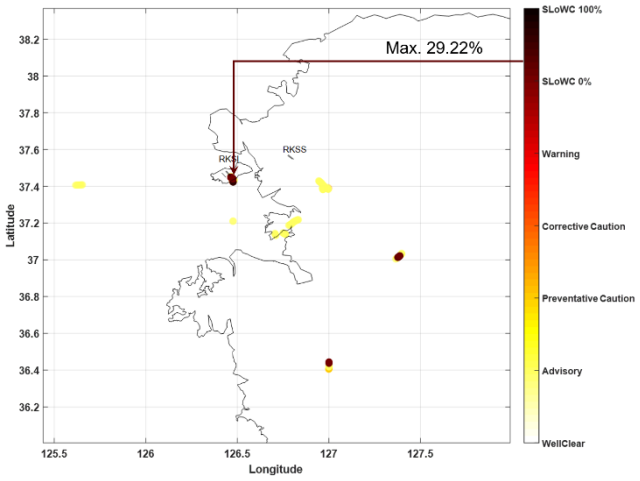

Fig. 22 LoWC and SLoWC - Factor 1.0 (April 21st, 2017)

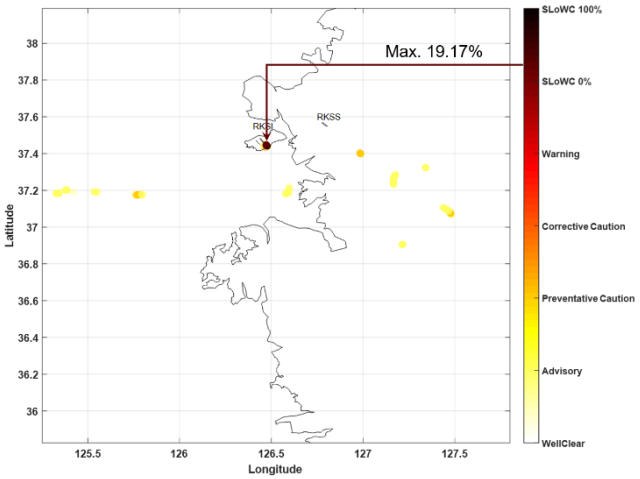

Fig. 23 LoWC and SLoWC - Factor 1.0 (April 22nd, 2017)

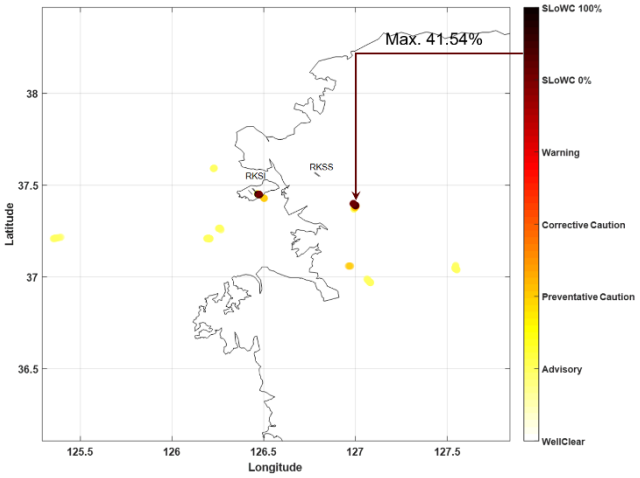

Fig. 24 LoWC and SLoWC - Factor 1.0 (April 23rd, 2017)

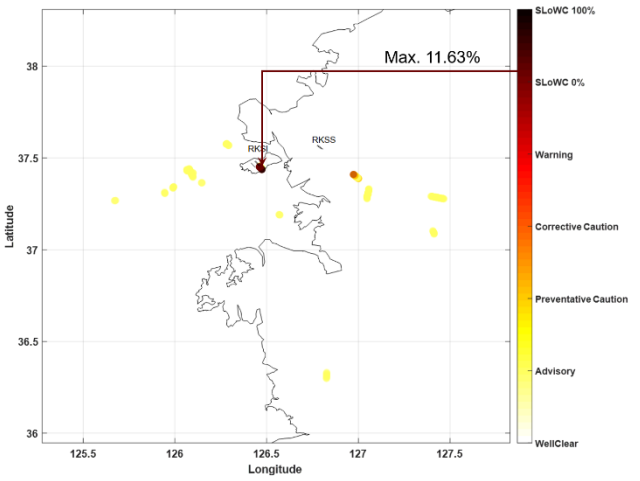

Fig. 25 LoWC and SLoWC - Factor 1.0 (April 24th, 2017)

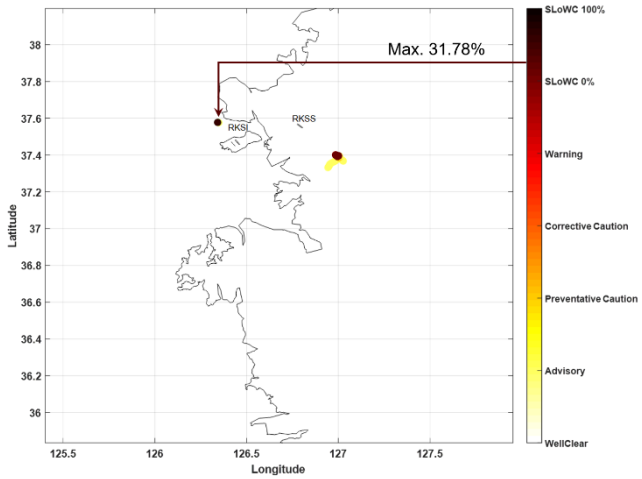

Fig. 26 LoWC and SLoWC - Factor 1.0
(April 25th, 2017)

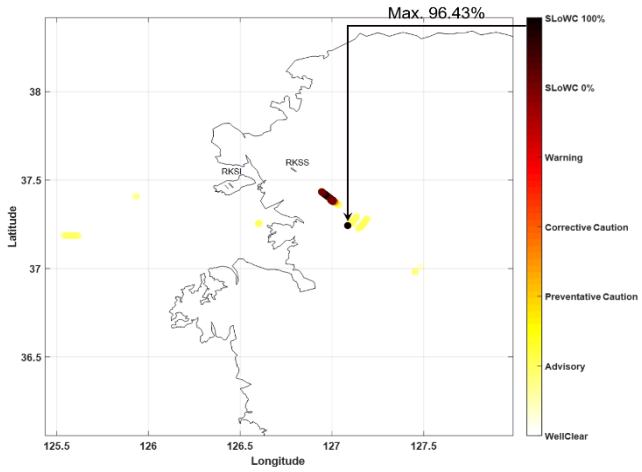

Fig. 27 LoWC and SLoWC - Factor 1.0
(April 26th, 2017)

4. Conclusion

Risks were analyzed by calculating CIP and WC of aircraft in Seoul TMA using a weeklong ADS-B data. Some of the potential risk area were identified, which were concentrated around the airport and the route merge points. In this busy airspace that contains two Class B airports, WC better represented the actual risk levels compared to CIP. Using relaxation factor showed its usefulness by providing relative intensity of the risk levels in the low risk areas.

The methodology developed in this paper will serve as bases for evaluating the various next generation air traffic management concepts by quantitatively stating the level of risk. The results shown in this paper can be especially valuable for unmanned aircraft integration effort [7] by providing not only risk analyses but also guideline for designing new routes and airspaces.

Acknowledgement

This work was supported by the Flight Safety Regulation Development, and Integrated Operation Demon for Civil UAS (No. 16ATRP-C108186-02) project under the Aviation Safety Technology Development Program funded by the Ministry of Land, Infrastructure and Transport (MOLIT), Republic of Korea.

References

[1] Lee H., Park, B., and Lee, H., “Waypoint Extraction from Recorded ADS-B Trajectory Data”, 2016 The Korean Navigation Institute Conference, KONI, Vol. 20, No. 1, 2016, pp. 194–196.

[2] Bilimoria, K., and Hilda Q., "Properties of air traffic conflicts for free and structured routing", AIAA Guidance, Navigation, and Control Conference, 2001, pp. 259-266.

[3] Jeong, S., Oh, H., Choi, K., and Lee, H., “Comparative Study of Conflict Detection Techniques in the Terminal Maneuvering Area”, 2015 KSAS Fall Conference, KSAS, 2015, pp. 475–478.

[4] Kang, J., Kang, S., Oh, H., Choi, K., Lee, H. T., Jung, H. T., and Moon, W. C., “Human-in-the-Loop Simulation of Trajectory Based Operation Concept for Remotely Piloted Aircraft System Integration”, In AIAA Modeling and Simulation Technologies Conference, 2017, p. 0806.

[5] Cook, S., and Brooks, D., “A Quantitative Metric to Enable Unmanned Aircraft Systems to Remain Well Clear”, Air Traffic Control Quarterly, 2015, pp. 137-156.

[6] Cone, A. C., Thipphavong, D., Lee, S. M., and Santiago, C., “UAS Well Clear Recovery against Non-Cooperative Intruders using Vertical Maneuvers”, In 17th AIAA Aviation Technology, Integration, and Operations Conference, 2017, p. 4382.

[7] Consiglio, M., Chamberlain, J., Munoz, C., and Hoffler, K., "Concept of Integration for UAS Operations in the NAS," In Proceedings of the International Congress of the Aeronautical Sciences, 2012.